# Geochemical vectoring for Skorpion (sulphide) and Rosh Pinah targets in the Gariep Belt, Namibia

S.J. Theron
*Exxaro Resources Ltd*

The Skorpion Zn oxide deposit is underlain by a Zn-Pb±Cu sulphide body, which is predominantly characterized by disseminated and stringer sulphide mineralization with relatively low base metal grades. This low-grade sulphide body is the source of the zinc concentrated in the Skorpion Zn-oxide deposit. The Skorpion Zn oxide deposit would thus not have formed without the underlying sulphide precursor. The understanding of this sulphide system is therefore of the utmost importance, as it might be the key to discovering other Skorpion-type Zn oxide and Rosh Pinah-type Zn-Pb±Cu sulphide deposits in the Gariep Belt in Namibia and South Africa, as well as within other volcanogenic massive sulphide (VMS) mineral belts throughout the world.

A mineralogical and geochemical characterization and vectoring study was initiated during ongoing exploration in the Skorpion–Rosh Pinah area to develop possible geological and geochemical vectors that would point the exploration teams in the direction of possible new sulphide bodies.

A bimodal volcanic horizon had been identified as a possible 'fertile' horizon by early exploration teams even before the discovery of the Skorpion Zn oxide deposit in the 1980s. The bimodal volcanic horizon is characterized by continental tholeiitic basalts and near-peralkaline rhyolite lavas and volcaniclastics. In contrast to the basaltic flows, the rhyolites do not seem to be restricted to the bimodal volcanic horizon, but in the Skorpion area also occur interlayered/interbedded with the immediately overlying sediments. This is quite important, as the base metal-bearing brine responsible for the sulphide mineralization appears to have been a high-temperature hydrous fluid directly related to the rhyolitic volcanism.

The Skorpion base metal sulphide mineralization is hosted by a string of lithologies, which include meta-basalts, meta-rhyolites, and siliciclastic and chemical sediments. The latter are dominated by limestones and impure limestones, but siliceous chemical sediments (cherts) also form an important part of the mineralized system. The siliciclastic sediments include mainly arkose to arkosic arenite to wackes and muscovite-rich, intensely tectonized greenschist metamorphosed versions thereof. All the lithologies hosting the base metal sulphide mineralization have been altered by the hydrothermal base metal-bearing brine. Quantifying the intensity of this hydrothermal alteration may be the solution to effective geochemical vectoring.

A geochemical method to distinguish between siliciclastic ± siliceous chemical sediments and rhyolite lava/volcaniclastics/hypabyssal intrusives has been developed. The rhyolite volcanics can be geochemically distinguished from the sediments using incompatible immobile trace elements and element ratios (*viz*. Ti, Zr, Y, V, Ta, P, Zr/Ti, Nb/Y, $La_N/Yb_N$, Hf/Ta, REE signature).

At least two groups of rhyolites have been identified, with the Group 1B rhyolites representing a possible 'fertile' near-peralkaline rhyolite suite, spatially and probably genetically associated with the base metal sulphide mineralization. This group is characterized by a unique incompatible trace element geochemical signature *viz*. (i) very pronounced negative Eu anomalies, (ii) flat chondrite-normalized REE patterns (low $La_N/Yb_N$ ratios), probably due to HREE enrichment (high $Yb_N$ values), (iii) sporadic LREE depletion and associated positive Ce anomalies, (iv) low Zr/Y and Nb/Y ratios as well as low $TiO_2$ and high Y values, and (v) generally complex REE patterns, similar to some peralkaline rhyolites.

The inherent magmatic characteristic of these rhyolites was modified by a later, but related, hydrothermal event that caused the wall-rock alteration (mainly increase in K, Ba,

±Fe and ±Si) and associated base metal mineralization (mainly Zn, Pb, Cu, S, Ag, Cd, Mo, Sb, Bi, Tl etc.). This caused the already pronounced negative Eu anomalies to become even more pronounced, possibly indicating that the metal-bearing hydrothermal fluid was derived from the hydrous magmatic fluids associated with the felsic volcanism and associated sub-volcanic magmatism. In contrast to other VMS deposits, circulating seawater cells played a negligible role in the creation of these orebodies. The lack of any significant Mg alteration (chlorite) is quite indicative of the lack of seawater influence.

Base metal (Zn-Pb±Cu) mineralization coincided with the introduction of K, Ba, ±Si, ±Fe, and ±Mn, and the simultaneous depletion in particularly Na, ±Ca and ±Mg. Enrichment in trace elements such as Rb, Tl, W, Mo, Bi, Cd, Ag etc. and depletion in especially Sr are associated with the latter. Remobilization and relative enrichment of Fe and Si is also quite evident.

Various major element alteration indices (AIs), based mainly on the enrichment in $K_2O$, BaO, and FeO, and depletion in $Na_2O$, ±CaO, and ±MgO, were formulated. They have been proposed as possible geochemical vectors if used in conjunction with each other or with trace elements and trace element ratios.

The altered and mineralized material is also anomalous in trace elements and trace element ratios, such as Tl, Bi, Rb, Ba/Sr, Rb/Sr, Eu/Eu*, total base metals (Zn+Pb+Cu), Cd, Y, $Yb_N$, Zr/Y, $La_N/Yb_N$, Mo, Sb, S.

## Introduction

The Skorpion Zn oxide deposit is underlain by a Zn-Pb±Cu sulphide body, which is characterized predominantly by disseminated and stringer sulphide mineralization with relatively low base metal grades. This low-grade sulphide body is the source of the zinc concentrated in the Skorpion Zn oxide deposit. The Skorpion deposit would thus not have formed without the underlying sulphide precursor. The understanding of this sulphide system is therefore of the utmost importance, as it might be the key to discovering other Skorpion-type Zn oxide and Rosh Pinah-type Zn-Pb±Cu sulphide deposits within the Gariep Belt in Namibia and South Africa, as well as within other volcanogenic massive sulphide (VMS) mineral belts throughout the world.

A mineralogical and geochemical characterization and vectoring study was initiated during ongoing exploration in the Skorpion–Rosh Pinah area to develop possible geological and geochemical vectors that would point the exploration teams in the direction of possible new sulphide bodies.

A bimodal volcanic horizon had been identified as a possible ‘fertile’ horizon by early exploration teams even before the discovery of the Skorpion Zn oxide deposit in the 1980s. The bimodal volcanic horizon is characterized by continental tholeiitic basalts and near-peralkaline rhyolite lavas and volcaniclastics. In contrast to the basaltic flows, the rhyolites do not seem to be restricted to the bimodal volcanic horizon, but in the Skorpion area also occur interlayered/interbedded with the immediately overlying sediments This is quite important, as the base metal-bearing brine responsible for the sulphide mineralization appears to have been a high-temperature hydrous fluid directly related to the rhyolitic volcanism (Frimmel *et al*., 1996; Leblanc *et al*., 1993 and Carvalho *et al*., 1999).

The Skorpion base metal sulphide mineralization is hosted by a string of lithologies, which include meta-basalts, meta-rhyolites, siliciclastic and chemical sediments. The latter are dominated by limestones and impure limestones, but siliceous chemical sediments (cherts) also form an important part of the mineralized system. The siliciclastic sediments include mainly arkose to arkosic arenite to wackes and muscovite-rich, intensely tectonized greenschist metamorphosed versions thereof. All the lithologies hosting the base metal sulphide mineralization have been altered by the hydrothermal base metal-bearing brine. Quantifying the intensity of this hydrothermal alteration may be the solution to effective geochemical vectoring.

## Geochemical characterization and development of geochemical vectors

As the Skorpion–Rosh Pinah sulphide mineralization appeared to be related to a hybrid volcanogenic massive sulphide–sedimentary-hosted exhalative (VHMS-SEDEX) system it was appropriate to initially apply standard vectoring tools such as the alteration box plot for VHMS systems (Large *et al*., 1998, 2001). This plot is made up of the Ishikawa alteration index (AI) plotted against the chlorite-carbonate-pyrite index (CCPI), with:

$$\mathbf{AI} = \frac{(K_2O + MgO)}{(K_2O + MgO + Na_2O + CaO)} \times 100$$

and

$$\textbf{CCPI} = \frac{(MgO + FeO)}{(MgO + FeO + Na_2O + K_2O)} \times 100$$

This alteration box plot has been previously used with great success in other areas where typical VHMS alteration was detected in the felsic lavas and volcaniclastics hosting Cu mineralization.

In the Skorpion–Rosh Pinah area only the ryolites and amphibolites are suited for the alteration box plot (Large *et al.*, 2001), as the alteration box plot geochemical vector was designed for only rocks with a rhyolite, dacite, and andesite-basalt composition. Felsic volcanics are also preferred, as alteration trends in mafic volcanics, such as basalts (amphibolites) cannot be as clearly defined as in felsic volcanics. Development of customized alteration indices specifically for the Skorpion–Rosh Pinah area was eventually attempted.

***Rhyolite volcanics***

*Alteration box plot*

The original igneous character of the rock is extremely important and needs to be known before the alteration box plot is used. Owing to the complicated geochemical, mineralogical, and petrographic characteristics of the rhyolites, siliciclastic sediments, siliceous exhalites, and tuffaceous exhalites (mixed sediments) major elements such as $SiO_2$, $K_2O$, $Na_2O$, CaO etc. could not be used to identify and classify the rhyolites. Only incompatible, immobile trace elements and element ratios (*viz*. Ti, Zr, Hf, Y, V, Ta, P, Nb/Y, $La_N/Yb_N$, Hf/Ta, Zr/Ti, REE signature) could successfully distinguish between the various siliceous rocks.

Zr, Ti, Ta, Hf, V, and ±P are the elements that unequivocally separate the rhyolites from the various sedimentary rocks. Hallberg's (1984) Ti *versus* Zr discrimination diagram for igneous rocks (Figure 1) indicates that the rhyolites clearly plot within the rhyolite field, while the sediments (arkoses, arenites, carbonaceous shale, quartz-muscovite schists, siliceous 'exhalites', and siliceous 'tuffaceous exhalites') concentrate along the dacite-andesite boundary and the biotite schists, biotite-amphibole schists, and amphibolites plot within the basalt field. The various rock types are thus clearly distinguished using Ti and Zr. The rhyolites are also depleted in V and enriched in Ta and Hf compared to the other rocks (Figures 2 and 3).

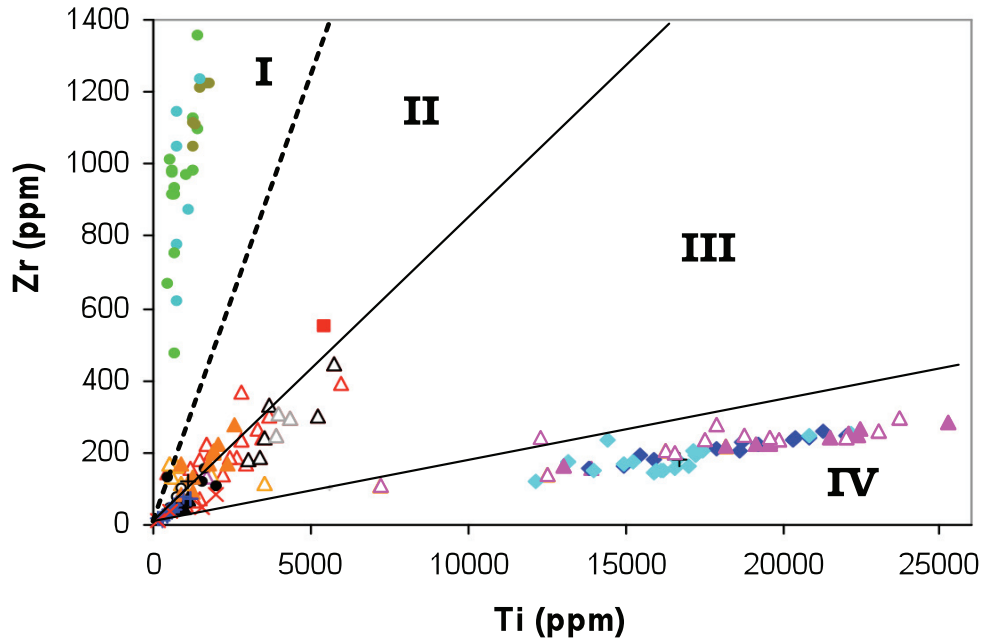


***Figure 1. Ti versus Zr discrimination diagram for extrusive igneous rocks (modified after Hallberg, 1984). The rhyolites (green, olive green, and blue circles) plot within the rhyolite field (I). The sediments, viz. arkoses (red open triangles), black shales (black open triangles), arkose-black shales (grey open triangles), siliciclastic arkoses-arenites (orange triangles), quartz-muscovite schists (open orange triangles), and siliceous sediments (tuffaceous exhalites and exhalites) (black circles) plot along the dacite (II) – andesite (III) boundary. The biotite schists (open purple triangles), biotite-amphibole schists (dark blue diamonds), and amphibolites (light blue diamonds) plot within the basalt field (IV)***

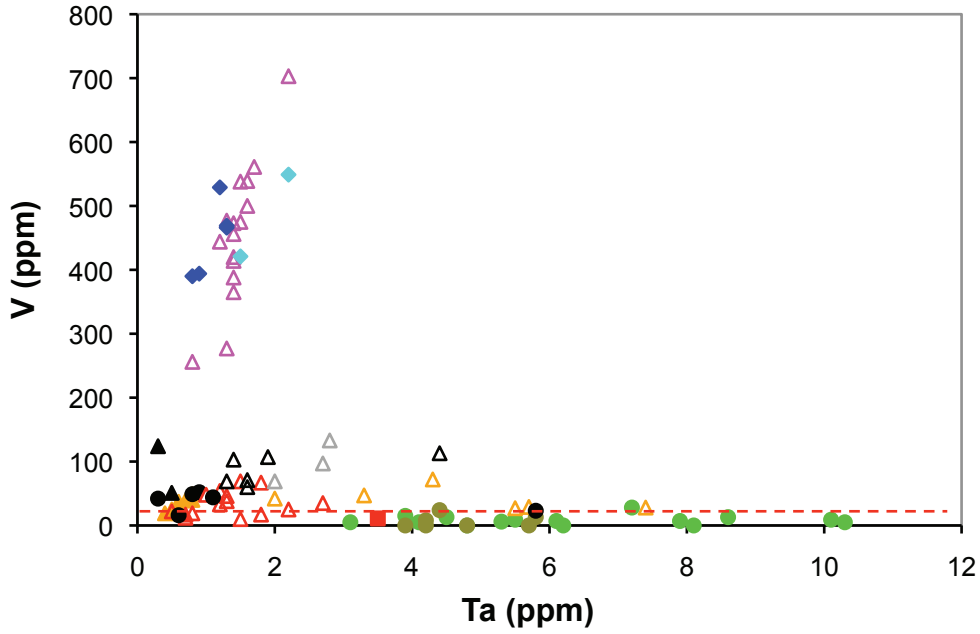


***Figure 2. Ta versus V diagram (A). The rhyolites (green and olive green circles) are relatively enriched in Ta and depleted in V. The biotite schists (open purple triangles), biotite-amphibole schists (dark blue diamonds), and amphibolites (light blue diamonds) are highly enriched in V and relatively depleted in Ta (mostly <2 ppm). For complete legend see Figure 1***

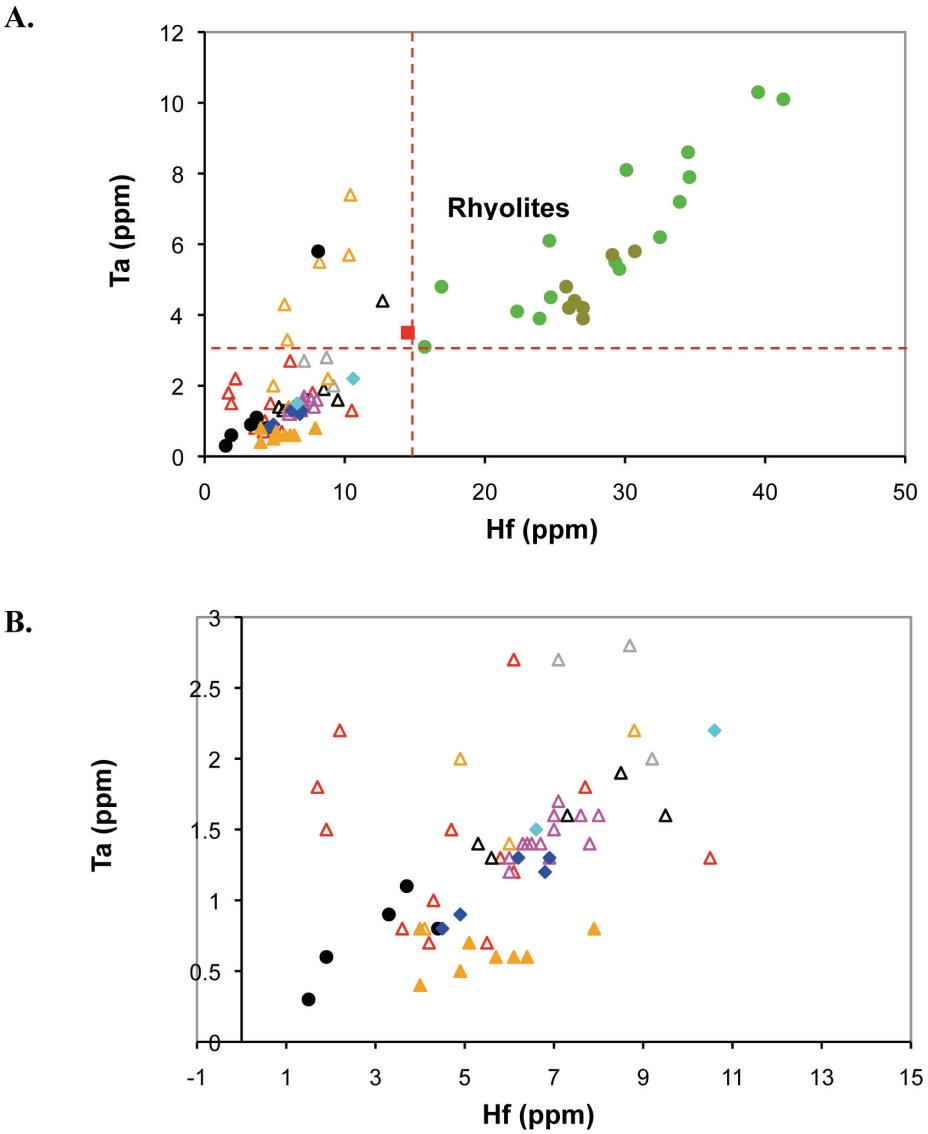


***Figure 3. (A) Hf versus Ta diagram. The Group 1 rhyolites (green circles) and Group 2 rhyolites (olive green circles) are enriched in Ta and Hf compared to the other rocks. Some of the quartz-muscovite schists (open orange triangles) and occasional black shales (open black triangles) and siliceous sediments (tuffaceous exhalites and exhalites) (black circles), also exhibit elevated Ta values. For complete legend see Figure 1. (B) Enlarged area (Hf 0 – 15 ppm and Ta 0–3 ppm) of Figure 3A***

The quartz-muscovite schists, tuffaceous exhalites, and black shales, however, are also sporadically enriched in Ta and depleted in V. The quartz-muscovite schists and siliceous tuffaceous exhalites both possibly represent mixed sediments. They may contain a rhyolitic volcaniclastic component, which causes these elevated Ta values. The rhyolites, siliceous tuffaceous exhalites and exhalites, quartz-muscovite schists, and some of the mineralized arkoses (Skorpion Zn oxide body) are relatively depleted in P (mostly < 450 ppm) and $TiO_2$ (mostly <0.3 wt.%) (Figure 4).

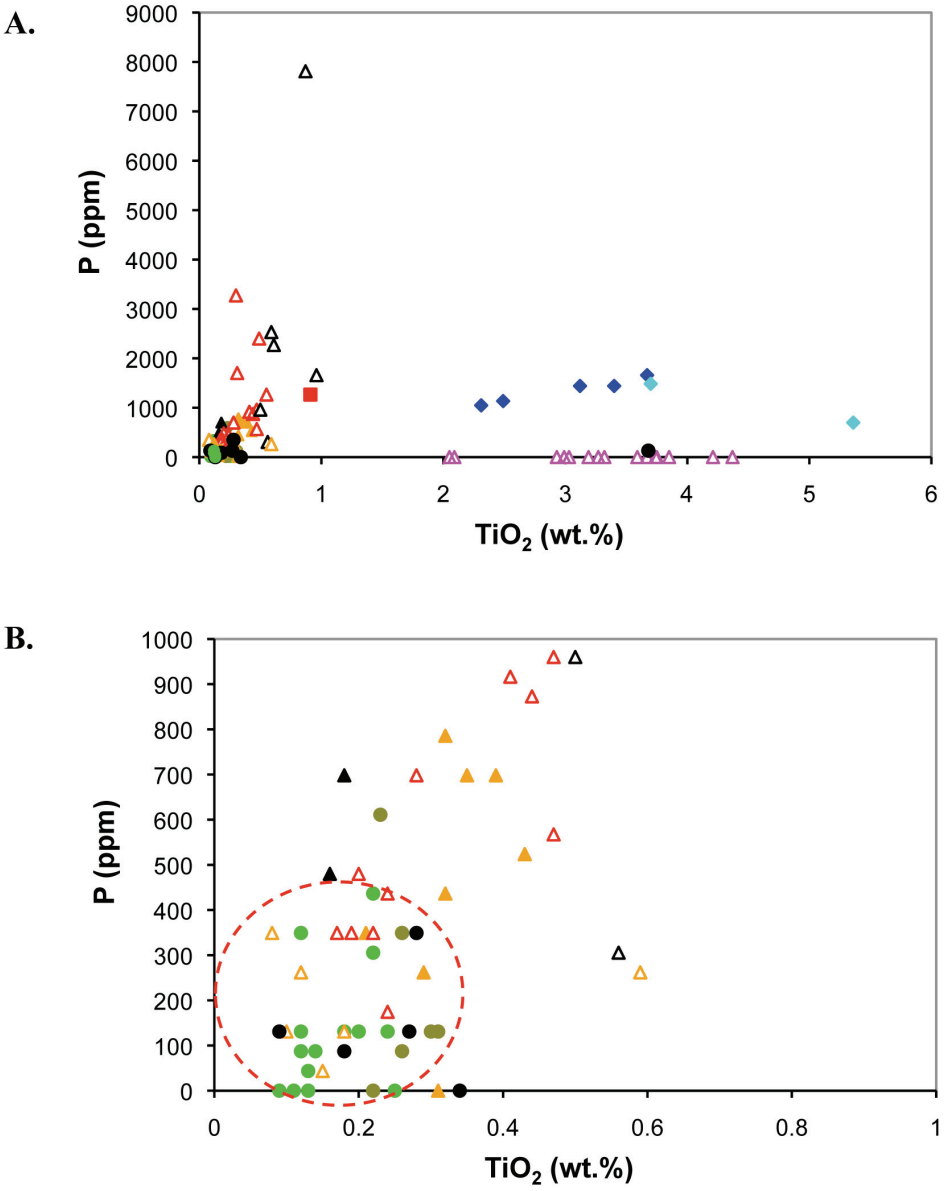


***Figure 4. (A) $TiO_2$ versus P diagram. The Group 1 (green circles) and Group 2 rhyolites (olive green circles) are relatively depleted in P and $TiO_2$ compared to the other rocks. Only the siliceous sediments (tuffaceous exhalites and exhalites) (black circles), quartz-muscovite schists (open orange triangles), and some of the arkoses (red open triangles) exhibit the same P and $TiO_2$ contents. For complete legend see Figure 1. (B) Enlarged area ($TiO_2$ 0–1 (wt.%) and P 0–1000 ppm) of Figure 4A***

Once the rhyolites are plotted on the alteration box plot (Large *et al.*, 2001) some of them appear unaltered ($2.0>Na_2O<5.0$ wt.%) and plot within the least altered rhyolite box (AI = 20 to 65 and CCPI = 15 to 45) (Figure 5). Three trends away from the least altered rhyolites can be observed, namely:

*Trend 1.* Some rhyolites may have been slightly altered by metamorphic albitization and plot toward albite (Figure 5).

*Trend 2.* Some of the rhyolites plot toward K-feldspar and/or sericite. This clearly indicates enrichment in potassium, particularly in the form of K-feldspar, and to a lesser extent sericite. The potassium enrichment in these rhyolites is probably due to K-metasomatism and Na-leaching associated with hydrothermal alteration (Figure 5).

*Trend 3.* A large proportion of rhyolites plot from K-feldspar and/or sericite toward the chlorite-pyrite 'ore centre'. The trend, however, ends one-third of the way towards the latter and the mineralized rhyolite samples from the Skorpion sulphide body do not plot within, or even close to, the 'ore centre' defined by Large *et al.* (2001). However, the mineralized rhyolites plot at the end of a strong trend towards this 'ore centre'. This trend is explained by an increase in FeO in the rhyolites due to the presence of Fe-rich (pyrite) and Fe-bearing sulphides (sphalerite).

Although some of the rhyolites do not contain any base metals and are thus officially not part of the Skorpion sulphide body, they are highly enriched in pyrite and are closely associated with the mineralized rhyolites from the Skorpion sulphide body (Figure 5). These pyrite-rich rhyolites may form part of a hydothermal alteration halo surrounding the base metal-rich Skorpion sulphide body.

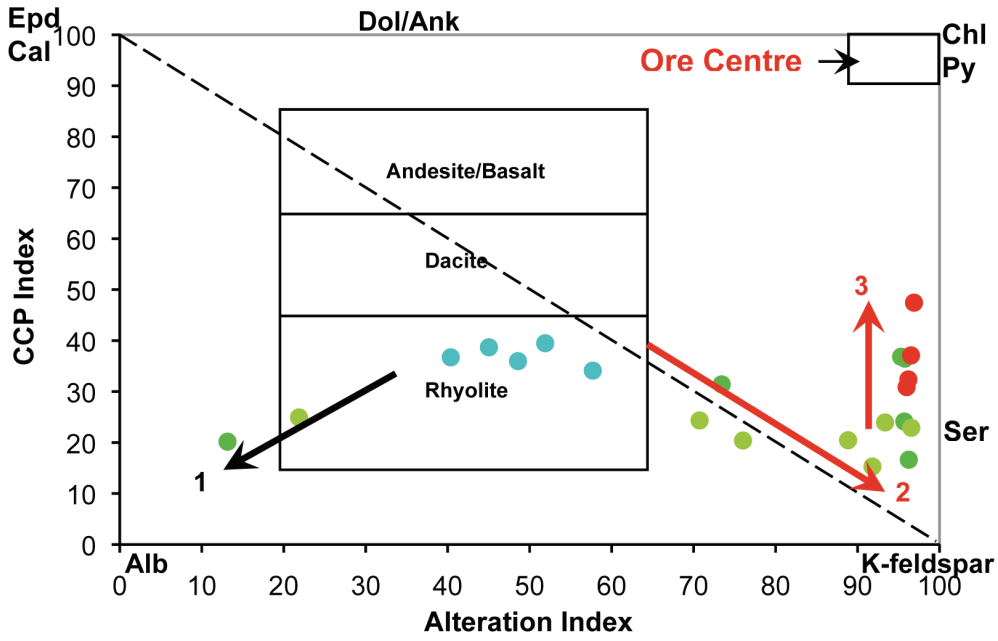


***Figure 5. Alteration box plot after Large et al. (2001). Three trends away from the least altered rhyolite box can be recognized. The first (1) towards the albite corner, the second (2) towards the K-feldspar corner, and the third (3) from the K-feldspar corner to the ore centre or chlorite-pyrite corner. Trends (2) and (3) are caused mainly by the hydrothermal enrichment in K-feldspar and Fe sulphides (pyrite) in the hydrothermally altered rhyolites. Least altered rhyolites (blue circles); altered Group 1 rhyolites (green circles); altered Group 2 rhyolites (olive green circles); mineralized rhyolites (red circles)***

Although the potassic (K-feldspar±sericite) and pyritic alteration characterizing the altered rhyolites are identified by the alteration box plot, the 'ore centre' defined by Large *et al.* (2001) is never reached. This is because the 'ore centre' in the alteration box plot is predominantly characterized by chlorite, pyrite, and/or Fe-bearing base metal sulphides. This causes an enrichment of both MgO and FeO in and towards the latter. No chlorite alteration and no increase in associated MgO have, however, been observed in the rhyolites from the Skorpion sulphide body.

The rhyolites from the Skorpion sulphide body (SKP ore centre) are predominantly characterized by Ba-rich K-feldspar±sericite and Fe-rich and Fe-bearing sulphides, which cause enrichment in BaO, $K_2O$, and FeO. The alteration box plot for VHMS deposits is thus only partially applicable to the Skorpion–Rosh Pinah area. However, a very positive characteristic of the alteration box plot is the strong relationship between the geochemical alteration trends observed and the alteration mineralogy underlying these trends.

As the AI makes provision for the enrichment of $K_2O$ in the Skorpion rhyolites, it was plotted against Ba in an attempt to refine the alteration box plot geochemical vector (Figures 6). However, only the rhyolites associated the Skorpion sulphide body and associated base metal sulphides plot within the SKP ore centre. Although the AI appears to be quite applicable to the Skorpion situation, the opposite may be true for the CCPI index. CCPI values actually decrease in samples affected by possible K-metasomatism, as $K_2O$, a predominant factor in the Skorpion alteration, forms an integral part of the CCPI denominator.

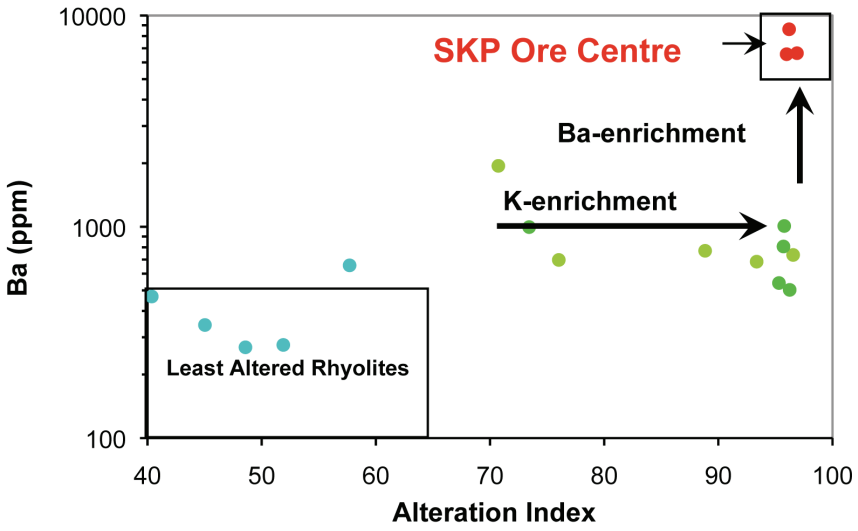


***Figure 6. Vectoring capabilities of the alteration box plot (Large et al., 2001) needs modification to make it applicable for the Skorpion mineralization. As the Skorpion sulphide base metal ore is highly enriched in Ba, Ba was added as another discrimination factor. In this diagram only the rhyolites directly associated with the base metal sulphide ore plot within the SKP ore centre.***

*Skorpion rhyolite alteration indices*

The AI and CCPI used to create the alteration box plot were modified in an attempt to create indexes and box plots more suited for the alteration observed in association with the Skorpion sulphide body. An increase in FeO, BaO, and $K_2O$ is commonly associated with the sulphide mineralization. Even the gossan at surface, which led to the discovery of the Skorpion oxide orebody and eventually the Skorpion sulphide body, is characterized by magnetite, pyrite, and barite. The magnetite and barite thus represent additional phases, not yet detected in the rhyolites, which indicate that an enrichment of Fe and Ba is associated with the base metal mineralization.

Four indexes to depict the enrichment in $K_2O$, BaO and FeO were tentatively formulated:

Skorpion rhyolite AI 1 (pyrite-magnetite AI):

$$\frac{(FeO)}{(FeO + MgO + Na_2O + CaO)} \times 100$$

Skorpion rhyolite AI 2A (K-feldspar AI):

$$\frac{(K_2O)}{K_2O + MgO + Na_2O + CaO)} \times 100$$

Skorpion rhyolite AI 2B (K-feldspar AI):

$$\frac{(K_2O + 10BaO)}{(K_2O + MgO + Na_2O + CaO)} \times 100$$

Skorpion rhyolite AI 3 (pyrite-feldspar-barite AI):

$$\frac{(FeO + 10BaO)}{(FeO + 10BaO + Na_2O + CaO + MgO)} \times 100$$

(For the Skorpion rhyolite AI 3 index, BaO is factored by 10, to bring its base value up to the magnitude of the other elements used.)

*Skorpion rhyolite AI 1 vs AI*

If the Skorpion rhyolite AI 1 is plotted against the AI (Skorpion alteration box plot 1), two trends away from the least altered rhyolites can be observed (Figure 7).

*Trend 1.* Similar to the alteration box plot; some samples may have been slightly altered by metamorphic albitization and plot toward albite (Figure 7).

*Trend 2.* For the Skorpion rhyolite AI 1, $K_2O$ (a predominant factor in the alteration associated with the Skorpion sulphide body) has been removed from the denominator in the CCPI. The enrichment in $K_2O$, represented by the Ishikawa AI along the x-axis, and the enrichment in FeO, represented by the Skorpion rhyolite AI 1 along the y-axis, cause a resultant trend towards the 'SKP ore centre' (Figure 7). The predominant reason is the presence of abundant K-feldspar and pyrite in these samples. Base metal suphides such as sphalerite, galena and chalcopyrite are, however, also present in the samples originating from the Skorpion sulphide body. Thus $K_2O$ and FeO increase and $Na_2O$ and CaO decrease in the hydrothermally altered rhyolites. Very little of the potassium enrichment is associated with sericite. No increase in chlorite, and thus in MgO, has been observed and the rhyolite rocks are, in fact, highly depleted in MgO, generally containing <0.5 wt.%. Some of the highly altered Group 1 rhyolites that plot within the 'SKP ore centre' due to high K and Fe, however, are not directly associated with the Skorpion sulphide body and are thus also not directly associated with the base metal sulphides (Figure 7). The rhyolites directly associated with the base metals are highly enriched in Ba – it therefore appears as if the K-feldspar ($K_2O$) and pyrite (FeO) halo around the Skorpion sulphide body could be much broader than the Ba and base metal halo.

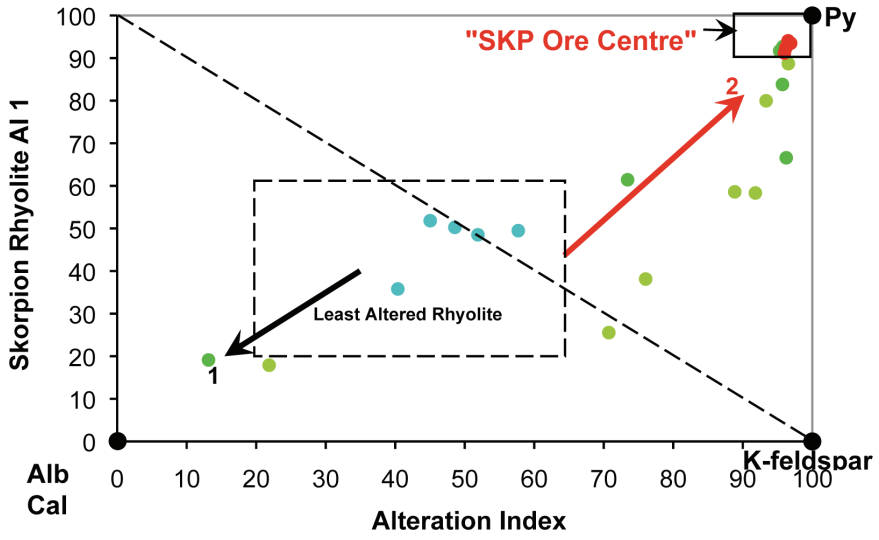


***Figure 7. The CCP index was modified to the Skorpion rhyolite AI 1 and a new Skorpion alteration box plot 1 was created. Two trends away from the least altered rhyolite box can be recognized. The first (1) towards the albite-calcite corner and the second (2) towards the 'SKP ore centre' or pyrite corner. Trend (2) is due to the enrichment in $K_2O$, represented by the Ishikawa alteration index, along the x-axis, and the enrichment in FeO, represented by the Skorpion rhyolite AI 1 along the y-axis. However, samples not directly associated with the base metal sulphide ore zone still plot within the 'SKP ore centre' box. For complete legend see Figure 5***

As the Skorpion rhyolite AI 1, similar to the AI and CCPI, does not make provision for the enrichment of BaO it was also plotted against Ba (Figure 8). As in the case of the AI (Large *et al.*, 2001) (Figure 6), only the rhyolites associated the Skorpion sulphide body and thus base metal sulphides plot within the SKP ore centre.

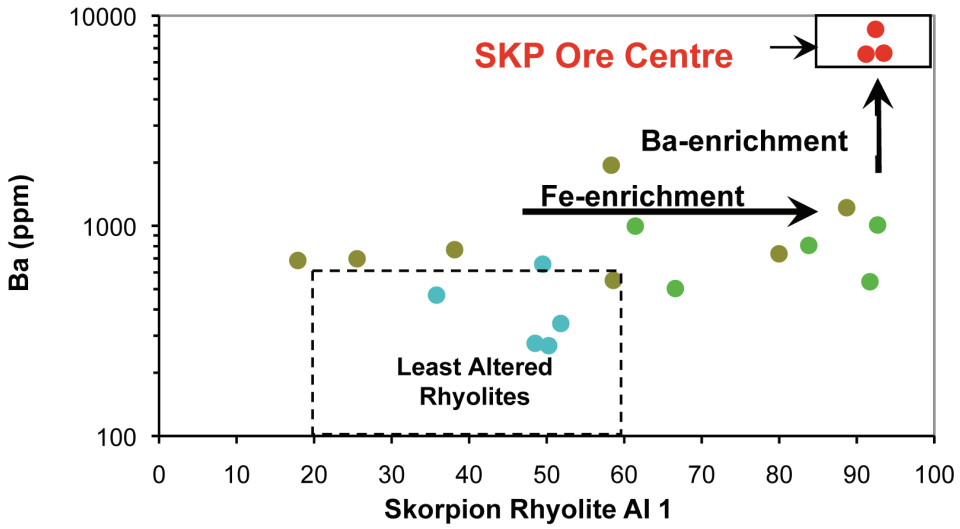


***Figure 8. Even the vectoring capabilities of the Skorpion alteration box plot 1 needs modification to make it more applicable to the Skorpion sulphide mineralization. As the Skorpion sulphide base metal ore is highly enriched in Ba, Ba was added as another discrimination factor. For complete legend see Figure 5***

*Skorpion rhyolite AI 3 vs AI or Skorpion rhyolite AI 2A*

The best results are achieved when the Skorpion rhyolite AI 3 is plotted against either the AI or Skorpion rhyolite AI 2A (Skorpion alteration box plot 2) (Figure 10). The Skorpion rhyolite AI 3 indicates enrichment in FeO and BaO relative to $Na_2O$, CaO, and MgO, and the AI enrichment in both $K_2O$ and MgO relative to $Na_2O$ and CaO, while the Skorpion rhyolite AI 2A indicates only enrichment in $K_2O$ relative to $Na_2O$, CaO, and MgO. The Skorpion rhyolite AI 3 makes provision for the enrichment in Ba. Thus only mineralized rhyolites from the Skorpion base metal sulphide body should plot within the SKP ore centre. Again, two trends away from the least altered rhyolites can be observed (Figure. 9).

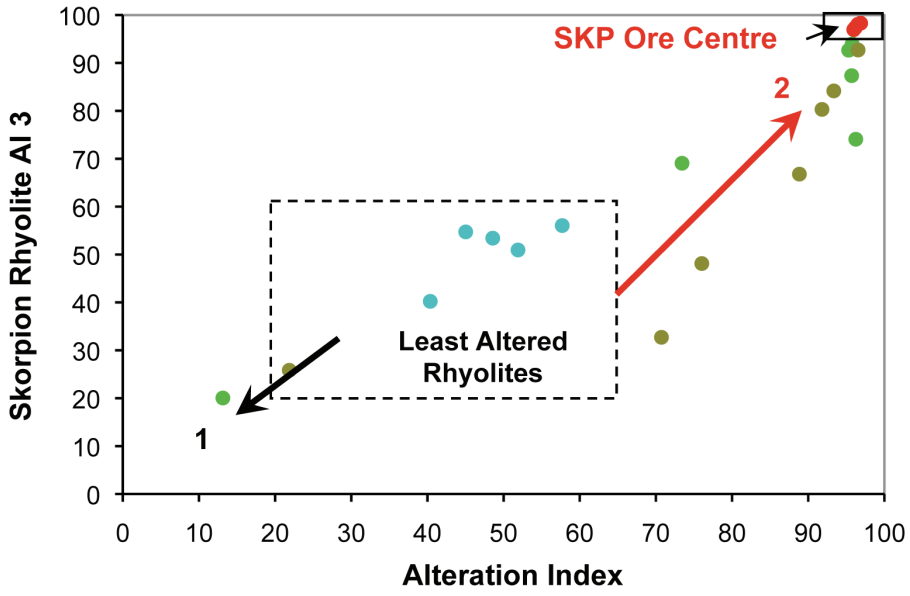


***Figure 9. The CCP index was modified to the Skorpion rhyolite AI 3 and a new Skorpion alteration box plot 2 was created. Again, two trends away from the least altered rhyolite box can be recognized. The first (1) towards the albite-calcite corner, and the second (2) towards the 'SKP ore centre' or pyrite corner. The latter is due to the enrichment in $K_2O$, represented by the Ishikawa alteration index, along the x-axis, and the enrichment in FeO and BaO, represented by the Skorpion rhyolite AI 3 along the y-axis. Now only samples directly associated with the base metal sulphide ore zone plot within the 'SKP ore centre' box. For complete legend see Figure 5***

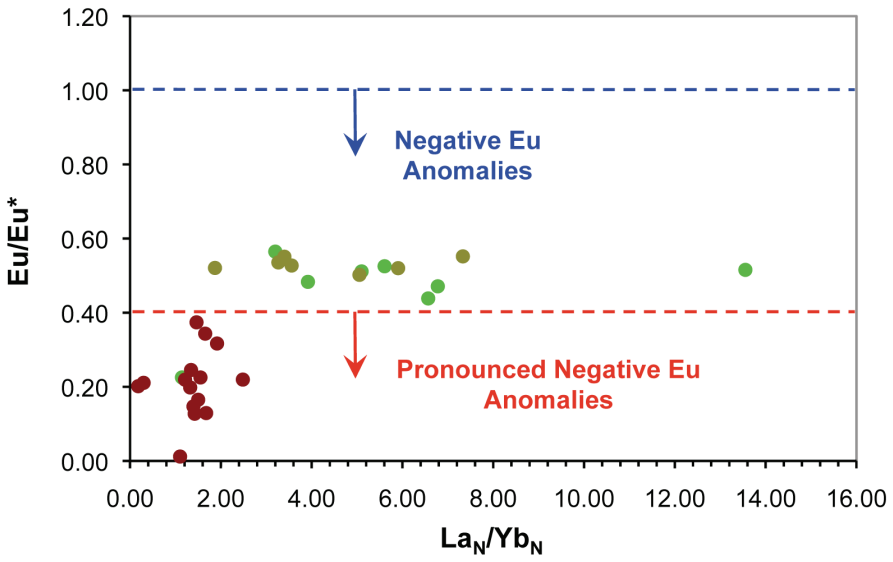


***Figure 10. A new classification of rhyolites was made based on their REE signatures. The 'fertile' Group 1B rhyolites (dark red circles) all originate from the immediate vicinity of the Skorpion orebody. Note their pronounced negative Eu anomalies and flat REE patterns (1.0 to 3.0 $La_N/Yb_N$ ratios). For complete legend see Figure 5***

Trend 1. Similar to the alterati on box plot (Large *et al*., 2001). Some samples may have been slightly altered by metamorphic albitization and plot toward albite (Figure 9).

Trend 2. Similar to the previous IA *vs* the Skorpion rhyolite AI 1 (Figure 7), this is a resultant trend towards the SKP ore centre due to the enrichment in $K_2O$, represented by the IA or the Skorpion Rhyolite AI 2A, along the x-axis, and the enrichment in FeO and BaO represented by the Skorpion rhyolite AI 3 along the y-axis (Figure 9). The predominant reasons for the enrichment in Fe, Ba, and K are the presence of abundant Ba-rich K-feldspar and Fe and Fe-bearing sulphides in the rhyolites from the Skorpion base metal sulphide ore body. The K and Fe halos, however, appears to be broader than the Ba and base metal halos; thus the combination of Ba with Fe in a ratio actually yields better results than the K-Ba combination (Skorpion rhyolite AI 2B).

*Rare earth element signatures*

At least two groups of rhyolites have been identified, with the group 1B rhyolites representing a possible 'fertile' near-peralkaline rhyolite suite, spatially and probably genetically associated with the base metal sulphide mineralization (Figure 10). These rhyolites are characterized by a unique incompatible trace element geochemical signature: (i) very pronounced negative Eu anomalies, (ii) flat chondrite-normalized REE patterns (low $La_N/Yb_N$ ratios), probably due to HREE enrichment (high $Yb_N$ values), (iii) sporadic LREE depletion and associated positive Ce anomalies, (iv) low Zr/Y and Nb/Y ratios as well as low $TiO_2$ and high Y values, and (v) generally complex REE patterns, similar to some peralkaline rhyolites (Bowden and Whitley, 1974).

These characteristics are independent of the degree of hydrothermal alteration and/or metasomatism and thus represent the inherent magmatic characteristic of the rhyolites (Figure 10). This group of rhyolites most probably represent a 'fertile' rhyolite suite consisting of highly differentiated/evolved alkali rhyolites, with the potential to be especially enriched in Zn. Not only the magmas, but also the hydrous fluids associated with these 'water-rich' magmas may be enriched in Zn.

This inherent magmatic characteristic was overprinted by a hydrothermal event that caused alteration (mainly K, Fe, and Ba) and base metal mineralization (mainly Zn, Pb, Cu, Ag, Cd, Bi, Tl etc.). This caused an intensification of the already pronounced negative Eu anomalies (Figure 10). This hydrothermal fluid may be closely associated with the hydrous magmatic fluids associated with the felsic volcanism and associated sub-volcanic magmatism (Lesher *et al*., 1986; Nicholls and Carmichael, 1969).

***Basaltic volcanics***

The biotite schists, biotite-amphibole schists, and amphibolites are all of a basaltic origin. Typical igneous textures characterized by interlocking plagioclase laths and needles and the characteristic Ti/Zr ratios indicate that all three of these rock types are related. Due to their similar Ti/Zr ratios and absolute Ti and Zr contents it is assumed that the

biotite schists, biotite-amphibole schists, and amphibolites rocks probably had the same composition before hydrothermal alteration, mineralization, and subsequent metamorphism. This composition was probably very close to that of the rocks currently classified as amphibolites. K, Ba, Rb, Tl, $SiO_2$, Fe, S, W, and Zn-Pb were added to the 'basaltic' system during hydrothermal alteration, resulting in the formation of biotite-quartz schists during coeval or subsequent metamorphism. Biotite ±garnet are the highest grade metamorphic minerals stable in these rocks, but they are of the same metamorphic grade as the biotite-amphibole schists and amphibolites. This probably indicates that the inherent K ±Si content of these biotite schists was higher than that of the biotite-amphibole schists and amphibolites before metamorphism. The biotite schist–biotite-amphibole schist–amphibolite series can thus be a very useful geochemical vector series.

*Petrological and geochemical characteristics of basaltic rocks*

Biotite schists

The biotite schists represent the most altered of these 'basaltic rocks' and are often closely associated with or host the base metal sulphide mineralization. The biotite-amphibole schists and amphibolites, although often anomalous in base metals, do not act as a major host to base metal sulphide mineralization. This, together with the geochemical and petrological evidence, indicates that the biotite schists represent metamorphosed products of K-metasomatised basaltic material.

K-metasomatism of the basaltic material was accompanied by enrichment in ±$SiO_2$, ±Ba, ±Rb, ±Zn, ±S, ±W, ±Tl, ±Fe etc. and depletion in Na, ±Ca, Sr, ±P etc.

The Ti/Zr ratios, as well as the absolute Ti and Zr values, indicate that the biotite schists, biotite-amphibole schists, and amphibolites essentially represent the same original rock material, namely basaltic volcanics (Figure 1), which were probably deposited in various forms (lavas, volcaniclastics, and possibly even subvolcanic/hypabyssal sills/dykes).

The mineralogical composition of the biotite schists can vary widely (biotite-quartz-plagioclase-calcite-ilmenite, biotite-quartz-K-feldspar-calcite-pyrite-ilmenite, biotite-muscovite-quartz-rutile-pyrite, biotite-muscovite-quartz-garnet (almandine-spessartine-grossularite)-rutile-barite-sphalerite-pyrite, biotite-quartz-ankerite ±calcite-ilmenite-pyrite-sphalerite, sphalerite-pyrite-siderite-biotite-muscovite-quartz etc.). Either ilmenite and/or rutile can be present – rocks are usually characterized by one or the other. The ilmenite is usually Mn- and Zn-bearing and has the potential to act as a very useful resistate indicator mineral in areas where these types of deposits are exposed. The massive sulphides hosted by calcareous biotite schists contain sporadic Fe carbonates, especially siderite.

The biotite schists are usually mineralized. In some cases, pyrite and pyrite after pyrrhotite are the dominant sulphides; in others sphalerite, galena, and traces of chalcopyrite accompany the pyrite. The sphalerite and galena are usually also more enriched in Ba than the rocks containing only pyrite and pyrite-magnetite after pyrrhotite. Barium is associated with barite, Ba-bearing K-feldspar, and Ba-bearing micas (biotite/muscovite).

These biotite schists can be divided into (i) intensely altered 'siliceous' biotite schists and (ii) slightly to moderately altered 'calcareous' biotite schists,

The intensely altered 'siliceous' biotite schists are characterized by enrichment in K, Ba, ±S, ±Si, ±Tl, W, ±As and base metals (Zn-Pb-Cu) and depletion in Na, Ca, Sr, and $CO_2$. The depletion of Ca, Sr, and $CO_2$ is related to the absence of calcite, while the depletion in Na is due mainly to the replacement of Na by K. The massive sulphides hosted by the biotite schists are, however, characterized by the presence of abundant Fe carbonates, especially siderite.

The slightly to moderately altered 'calcareous' biotite schists are characterized by variable enrichment in K, Si, S, Tl, and base metals (mainly Zn-Pb) and a depletion in Na. Calcite is a common constituent of these 'calcareous' biotite schists and the rocks are thus relatively enriched in Ca, $CO_2$, and Sr.

Biotite-amphibole schists

The biotite-amphibolite schists probably represent basaltic material slightly or moderately altered by the hydrothermal fluids. These schists are usually characterized by a foliate biotite-plagioclase-ilmenite ±magnetite ±quartz ±calcite matrix, with coarse poikiloblastic hypidiomorphic to idiomorphic amphibole porphyroblasts occurring throughout. The amphibole porphyroblasts transect the foliation and thus represent the highest metamorphic grade, post-peak tectonism mineral. Occasionally these amphibole porphyroblasts appear to be chemically unstable and are partly or completely replaced by later biotite. This indicates that, in some cases, due to the inherently higher K content of the rocks, the higher metamorphic grade amphiboles become 'unstable' and are replaced by 'stable' biotite. In some calcareous rocks the amphibole porphyroblasts are also completely pseudomorphically replaced by calcite.

Pyrrhotite, pyrite, and peripheral chalcopyrite are the dominant sulphides present and no sphalerite and/or galena have been detected.

These rocks are only slightly enriched in K and slightly depleted in Na, with no obvious enrichment in $SiO_2$, Ba, W etc.

Amphibolites

These rocks consist predominantly of amphibole, plagioclase, ilmenite, magnetite, ±calcite and ±quartz. The dark green to blueish-green amphiboles occur as a foliate mass and/or as distinct poikiloblastic porphyroblasts, the latter usually transecting the general foliation of the rock. The interstitial plagioclase often exhibits typical igneous textures, with euhedral to subhedral plagioclase laths and needles forming an interlocking mass. The plagioclase can also be recrystallized and can form a polygonal granoblastic mosaic interstitial to the amphibole, together with variable amounts of quartz. This polygonal granoblastic plagioclase-quartz mosaic may also exhibit a strong foliation/fabric parallel to those exhibited by the fibrous amphibole.

Lenticular laminae and mottles of coarse, elongated, and somewhat orientated polygonal granoblastic quartz and coarse augen-shaped structures filled with Fe-stained sparry calcite and polygonal granoblastic quartz commonly occur throughout these amphibolites.

Similar to the biotite-amphibole schists, pyrrhotite, pyrite, and peripheral chalcopyrite are the dominant sulphides present, and no sphalerite and/or galena have been detected.

The amphibolites are in some cases altered by epidotization and chloritization. The epidote predominantly replaces the calcic portion of the plagioclase and the chlorite usually replaces biotite and amphibole, but can also replace plagioclase together with calcite and epidote.

Ilmenite and variable amounts of magnetite are disseminated throughout these rocks.

Massive sulphides

The massive sulphides consist mainly of pyrite and sphalerite, with minor to accessory amounts of galena and traces of pyrrhotite and chalcopyrite. The sphalerite is Fe-rich and suffers from 'chalcopyrite disease', which is characterized by a multitude of very fine chalcopyrite inclusions/exsolutions occurring throughout the sphalerite. The Fe-rich nature of the sphalerite, as well as the presence of chalcopyrite disease, suggests that these sulphides formed at relatively high temperatures (probably 300°C to 450°C).

The main gangue phases associated with the sulphides are siderite, muscovite, quartz, and biotite. Barite, Ba-bearing K-feldspar, and rutile ±ilmenite are present in minor amounts. Minor traces of clinochlore, retrograde after biotite, are also sporadically present.

*Skorpion basaltic alteration indices*

Similar to the rhyolites from the Skorpion–Rosh Pinah area, the altered and mineralized basalts exhibit a distinct enrichment in K, Ba, and possibly Fe, and a distinct depletion in Na. These rocks are also characterized by a possible slight depletion in Ca and/or Mg. Six major element alteration indexes based on the latter were formulated:

Skorpion basalt AI 1 (biotite-buscovite):

$$\frac{(K_2O + FeO)}{(K_2O + FeO + Na_2O + MgO)} \times 100$$

Skorpion basalt AI 2 (mica-feldspar-barite):

$$\frac{(K_2O + 10BaO)}{(K_2O + 10BaO + MgO + Na_2O + CaO)} \times 100$$

Skorpion basalt AI 2A (mica-feldspar-barite):

$$\frac{(K_2O + 10BaO)}{(K_2O + 10BaO^{1} + Na_2O + CaO)} \times 100$$

(BaO is factored by 10, to bring its base value up to the magnitude of the other elements used)

Skorpion basalt AI 3 (pyrite-Fe-carbonate-barite):

$$\frac{(FeO + 10BaO)}{(K_2O + 10BaO + MgO + Na_2O + CaO)} \times 100$$

Skorpion basalt AI 4 (mica-feldspar):

$$\frac{(K_2O)}{(K_2O + MgO + Na_2O + CaO)} \times 100$$

General Skorpion basalt AI:

$$\frac{(K_2O+10BaO+FeO)}{(K_2O + 10BaO + FeO + MgO + Na_2O + CaO)} \times 100$$

Skorpion basalt AI 1 *vs* Skorpion basalt AI 2

If the Skorpion basalt AI 1 is plotted against the Skorpion basalt AI 2 (Skorpion basalt alteration box plot 1), a trend away from the least altered basalts (ortho-amphibolites) towards the SKP ore centre emerges. The Skorpion basalt AI 1 indicates enrichment in $K_2O$ and FeO relative to $Na_2O$ and MgO, and the Skorpion basalt AI 2 indicates enrichment in both $K_2O$ and BaO relative to MgO, $Na_2O$, and CaO (Figure 11). The ortho-amphibolites thus represent the least altered material, with Skorpion basalt AI 2 values varying between 0 and 13. The 'siliceous' biotite schists and associated massive sulphides represent the most intensely altered and mineralized basaltic material with Skorpion basalt AI 2 values, mostly varying between 72 and 97.

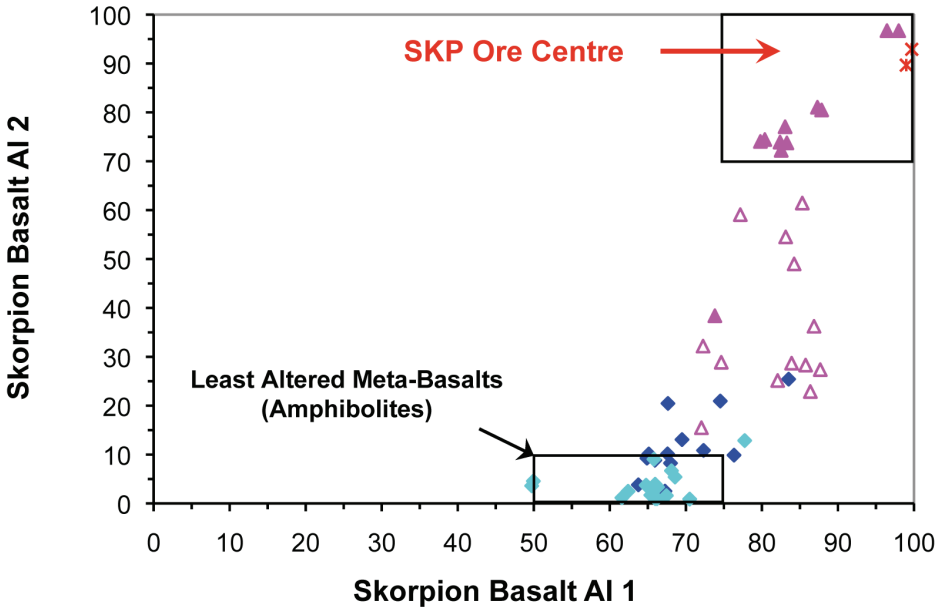


***Figure 11. Skorpion basalt alteration box plot 1, with the Skorpion basalt AI 1 versus the Skorpion basalt AI 2. A resultant alteration trend from the least altered meta-basalts (amphibolites) (light blue diamonds) to the most intensely altered and mineralized 'siliceous' biotite schists (closed pink triangles) and massive sulphides (red stars) is evident. For complete legend see Figure 1***

The Skorpion basalt AI 2 appears to be a very effective index, with the least altered material giving values below 13 and the intensely altered and mineralized material giving values from above 70 to close to 100 (Figure 11) .

Removing MgO from the denominator (Skorpion basalt AI 2A) increases the variance of the index values, with the least altered amphibolites reporting values of between 0 and 17, while the intensely altered 'siliceous' biotite schists exhibit values mostly between 95 and 100 (Figure 12).

The Skorpion basalt AI 1 exhibits a much smaller variance, as FeO forms an integral part of the index's numerator. The background values of iron within the unaltered basalts are much higher than that of potassium, and the index thus starts off at a much higher base. The least altered orthoamphibolites thus exhibit Skorpion basalt AI 1 values of between 62 and 71, while the altered biotite schists exhibit values mostly greater than 80 and the massive sulphides samples values close to 100 (Figure 11 and 12).

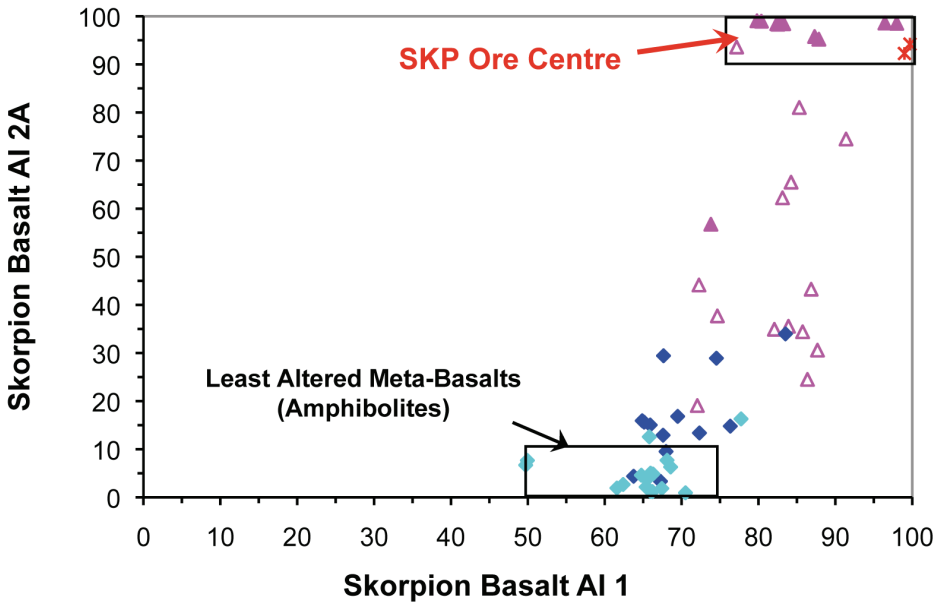


***Figure 12. Skorpion basalt alteration box plot 1A, with the Skorpion basalt AI 1 versus the Skorpion basalt AI 2A. An alteration trend from the least altered meta-basalts (amphibolites) (light blue diamonds) to the most intensely altered and mineralized 'siliceous' biotite schists (closed pink triangles) and massive sulphides (red stars) is evident. This trend is caused by the addition of K, Ba, and Fe to, and the depletion of particularly Na and ±Ca from, the hydrothermally altered meta-basalts. For complete legend see Figure 1***

Skorpion basalt AI 3 vs Skorpion basalt AI 4

As potassium occurs as numerator in both the Skorpion basalt AI 1 and 2, it obviously contributes to the linear trend observed in the Skorpion basalt alteration box plot 1 (Figure 11 and 12). The numerators of the Skorpion basalt AI 3 and 4 have thus been chosen specifically to buffer this linear mathematical effect.

Despite this, a resultant alteration trend away from the least altered basalts (ortho-amphibolites) towards the SKP ore centre also emerges in the Skorpion basalt alteration box plot 2 (Figure 13). The Skorpion basalt AI 3 index indicates enrichment in FeO and BaO relative to MgO, $Na_2O$, and CaO, and the Skorpion basalt AI 4 enrichment in $K_2O$ relative to MgO, $Na_2O$, and CaO (Figure 13). The ortho-amphibolites thus represent the least altered material, with Skorpion basalt AI 4 values varying between 0 and 10. The 'siliceous' biotite schists and associated massive sulphides represent the most intensely altered and mineralized basaltic material, with Skorpion basalt AI 4 values varying mostly between 50 and 69. The altered and mineralized 'calcareous' biotite schists are in general characterized by Skorpion basalt AI 4 values greater than 20 and smaller than 50, while the biotite-amphibole schists exhibit mostly values smaller than 20, and the ortho-amphibolites values mostly smaller than 5.

The Skorpion basalt AI 3 especially emphasizes the enrichment of FeO and BaO within the intensely altered and mineralized 'siliceous' biotite schists and associated massive sulphides, with these rocks exhibiting values of predominantly between 80 and 100 (Figure 13).

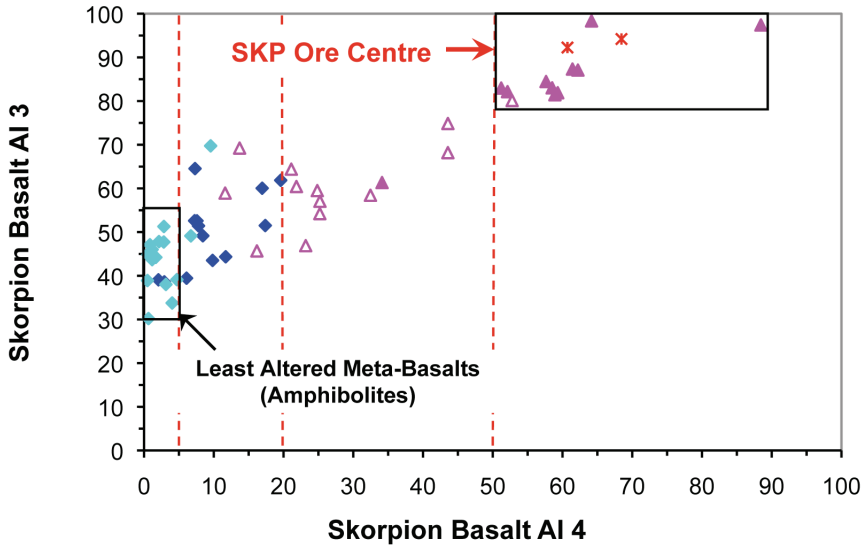


***Figure 13. Skorpion basalt alteration box plot 2, with the Skorpion basalt AI 4 versus the Skorpion basalt AI 3. An alteration trend from the least altered meta-basalts (amphibolites) (light blue diamonds) to the most intensely altered and mineralized 'siliceous' biotite schists (closed pink triangles) and massive sulphides (red stars) is evident. This trend is caused by the addition of K, Ba, and ±Fe to, and the depletion of particularly Na and ±Ca from, the hydrothermally altered meta-basalts. For complete legend see Figure 1***

General Skorpion basalt alteration index

The use of a general Skorpion basaltAI, which incorporates all the major element enrichments and depletions observed in the basaltic rocks, is proposed. This AI can be used in conjunction with trace elements and trace element ratios such as total base metals (Zn+Pb+Cu), Eu/Eu*, Ba/Sr, Tl, Bi+Tl, W, etc. (Figures 14 and 15).

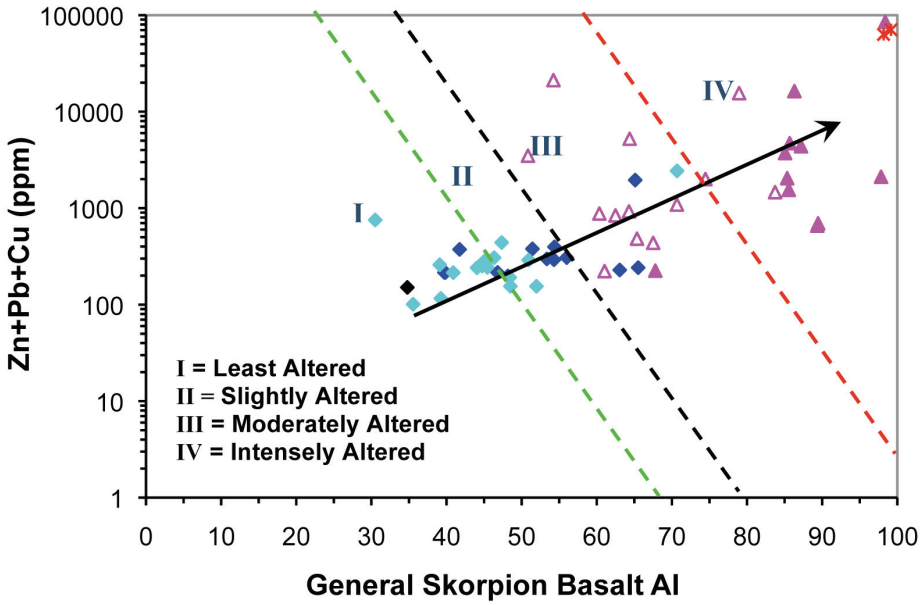


***Figure 14. General Skorpion basalt AI versus total base metals (Zn+Pb+Cu). An alteration trend from least altered amphibolites (light blue diamonds) to the most intensely altered and mineralized 'siliceous' biotite schists (closed pink triangles) and massive sulphides (red stars) is evident. The general Skorpion basalt AI thus accurately reflects the degree of alteration and mineralization within these rocks. For complete legend see Figure 1***

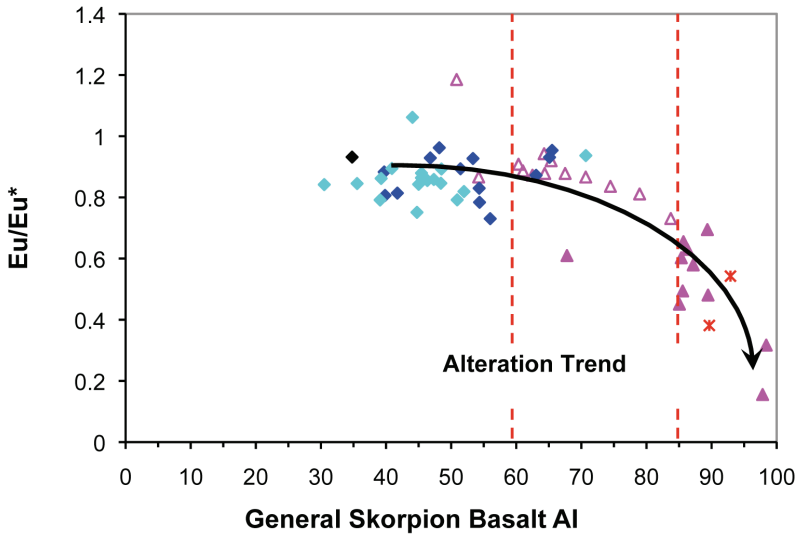


***Figure 15. General Skorpion basalt AI versus Eu/Eu* (<1 Eu/Eu* = negative Eu anomaly). An alteration trend from least altered amphibolites (light blue diamonds) to the most intensely altered and mineralized 'siliceous' biotite schists (closed pink triangles) and massive sulphides (red stars) is evident. The intensely mineralized rocks exhibit distinct negative Eu anomalies. For complete legend see Figure 1***

## Conclusions

The meta-basaltic and rhyolitic rocks from the Skorpion area have been geochemically charecterized according to their incompatible trace element content and element ratios such as Ti/Zr, Zr, and Ti.

A 'fertile' near-peralkaline alkali-rhyolite suite, characterized by a unique incompatible trace element geochemical signature has been identified. This signature includes very pronounced negative Eu anomalies; flat chondrite-normalized REE patterns, due to HREE enrichment; low Zr/Y and Nb/Y ratios (high Y values); and low $TiO_2$ content.

The hydrothermal fluid inherently had the same REE characteristics as these 'fertile' rhyolites, with all the intensely altered and mineralized host rocks exhibiting strong to pronounced negative Eu anomalies and flatter REE signatures compared to their unaltered or slightly altered equivalents.

As the 'fertile' rhyolite suite is interbedded/interlayered with the complete volcano-sedimentary package of rocks, economic Zn-Pb ±Cu mineralization can theoretically occur in any of the lithologies comprising that package. However, if Rosh Pinah is used as an example, the main host rock target should be the stratigraphically and/or structurally interbedded arkosic to arenitic siliciclastic sediment and limestone package overlying the volcanic-dominated horizon. The permeability and reactive nature of the siliciclastic sediments combined with the less permeable and reactive nature of the limestones may have made this package a more favourable host than the volcanic-dominated horizon.

The meta-basalts exhibit a very distinctive alteration trend from amphibolites to biotite-amphibole schists to slightly to moderately altered 'calcareous' biotite schists to intensely altered 'siliceous' biotite schists. Both the latter are characterized by K and Ba enrichment as well as base metal mineralization. It appears, however, as if the intensely altered 'siliceous' biotite schists are associated with the more intensely mineralized part of the system.

The biotite schists represent K-metasomatized, ±Ba-altered, ±silicified and ±mineralized (Zn ±Pb ±Cu ±Ag) meta-basalts, with the ortho-amphibolites representing the least altered meta-basaltic material. These biotite schists can be divided into two groups (i) slightly to moderately altered and mineralized 'calcareous' biotite schists and (ii) intensely altered and mineralized 'siliceous' biotite schists.

Fe carbonates, especially siderite, are associated with the massive sulphides from the Skorpion sulphide body. The highest grade base metal mineralization in the Rosh Pinah orebody is often also associated with siderite and ankerite, which represent an addition of Fe, Mg, and Mn to the system.

Several Skorpion/Rosh Pinah alteration indexes are proposed as possible geochemical vectors to alteration and associated mineralization. These alteration indexes are based on the addition of K, Ba, and ±Fe, and the simultaneous depletion of Na, ±Ca, and ±Mg from these rocks during hydrothermal alteration accompanying the base metal mineralization.

These major element alteration indexes can be used as possible vectors to mineralization in combination with each other or together with trace elements and trace element ratios. The latter include total base metals (Zn+Pb+Cu), Ba/Sr, Rb/Sr, Eu/Eu*, Tl, W, Y, Nb/Y etc. The total base metals, Eu/Eu*, Ba/Sr, and Tl in particular exhibit very useful alteration trends if used in conjunction with the major element alteration indexes.

**References**

Board, W.S. 1998. Fluid evolution within the outer margin of the Gariep Belt. PhD thesis, University of Cape Town. 175 pp.

Bowden, P. and Whitley, J.E. 1974. Rare-earth patterns in peralkaline and associated granites. *Lithos*, vol 7. pp. 15-21.

Carvalho, D, Barriga, F.J.A., and Munha J. 1999. Bimodal siliciclastic systems – the case of the Iberian Pyrite Belt. *Volcanic-associated Massive Sulfide Deposits: Progresses and Examples in Modern and Ancient Setting*. Barrie, C.T. and Hannington, M.D. (eds). *Reviews in Economic Geology*, vol. 8. pp. 375-408.

Frimmel, H.E., Hartnady, C.J.H., and Koller, F. 1996, Geochemistry and tectonic setting of magmatic units in Pan-African Gariep Belt, Namibia. *Chemical Geology*, vol. 130. pp. 101-121.

Hallberg, J.A. 1984. A geochemical aid to igneous rock identification in deeply weathered terrain. *Journal of Geochemical Exploration*, vol 20. pp. 1-8.

Large, R.L, Gemmell, J.B., and Herrmann, W. 1998. Summary of geochemical and mineralogical vectors to ore, based on the seven case studies in P439: CODES: AMIRA/ARC Project P430 – Studies of VHMS-related alteration: geochemical and mineralogical vectors to ore.

Large, R.L, Gemmell, J.B., and H. Paulick. 2001. The alteration box plot: a simple approach to understanding the relationship between alteration mineralogy and lithogeochemistry associated with volcanic hosted massive sulphide deposits. *Economic Geology*, vol. 96, no. 5. pp. 957-972.

Leblanc, M. 1993. A massive sulphide deposit formed below the sea floor and associated with felsic sills (Hajar, Morocco) *Proceedings of the Second Biennial SGA Meeting*, Granada, 9–11 September. Fenoll Hach-Ali, P., Torres-Ruiz, J., and and Gervilla, F. (eds). University of Granada. pp. 331-334.

Lesher, C.M., Goodwin, A.M., Campbell I.H., and Gorton, M.P. 1986. Trace-element geochemistry of ore-associated and barren, felsic metavolcanic rocks in the Superior Provice, Canada. *Canadian Journal of Earth Science*, vol. 23. pp. 222-237.

Nicholls, J. and Carmichael, J.S.E. 1969. Peralkaline acid liquids: a petrological study. *Contributions to Mineralogy and Petrology*, vol. 20. pp. 268-294.

**The Author**

**Salomon (Solly) Johannes Theron**, *Principal Mineralogist*, Exxaro Resources Ltd.

Graduated from RAU (now University of Johannesburg) with a M.Sc. in Geology in 1993. Joined Anglo American Research Labs in 1994 as a Mineralogist in the Gold and Base Metal Unit. In 1998 was transferred to Anglo Exploration and Acquisition Division as an Exploration Petrologist - Geochemist. Gained experience on gold and base metal deposits all over Africa. In 2003 was transferred to Anglo American Research Division as a Process Mineralogist. Joined Mintek in 2005 as Head of the Process Mineralogy Unit. Joined SGS South Africa in 2006, first as Technical Manager and later, in 2007, as Manager of Mineralogy. Gained experience on gold, PGE, base metal, uranium and industrial mineral related processing challenges. Joined Mintek as Chief Engineer in the Mineral Processing Division: Flotation Unit in 2011. Gained experience on processing of PGE, gold and base metal ores, especially with regard to flotation and comminution. Joined Exxaro Metallurgical R&D in 2012 as Principal Mineralogist, gaining experience on coal, related reductants and iron ore.